In situ characterization of battery materials using x-ray absorption spectroscopy

Carlo Segre

Physics Department
&
Center for Synchrotron Radiation Research and Instrumentation
Illinois Institute of Technology

March 6, 2018

Outline & Motivation

- Motivation

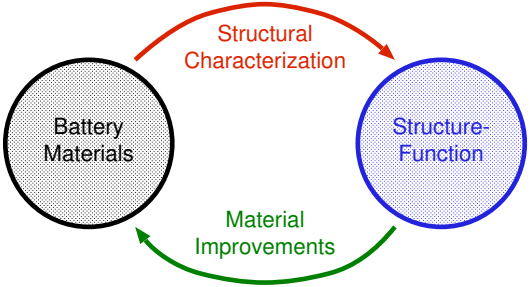

X-ray absorption spectroscopy provides element-specific view of both crystalline and amorphous phases with time resolution relevant to battery studies

Outline & Motivation

- Motivation
- X-ray absorption spectroscopy
- Application of XAS to batteries
- Ex situ study Mn-containing cathode
- In situ Ni@Co core shell cathode
- Sn_4P_3/graphite composite anode

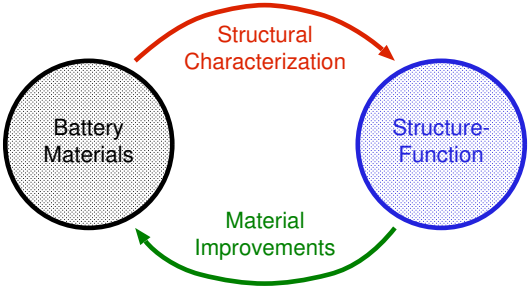

X-ray absorption spectroscopy provides element-specific view of both crystalline and amorphous phases with time resolution relevant to battery studies

The EXAFS experiment

I_o = incident intensity
I_t = transmitted intensity
I_f = fluorescence intensity
$\mu(E)$ = absorption coefficient

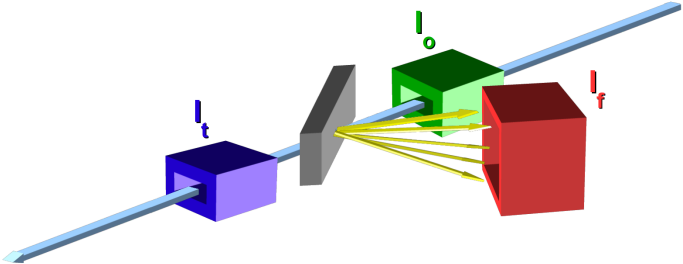

$$\mu(E) \propto \ln\left(\frac{I_o}{I_t}\right) \propto \frac{I_f}{I_o}$$

The EXAFS experiment

I_o = incident intensity
I_t = transmitted intensity
I_f = fluorescence intensity
$\mu(E)$ = absorption coefficient

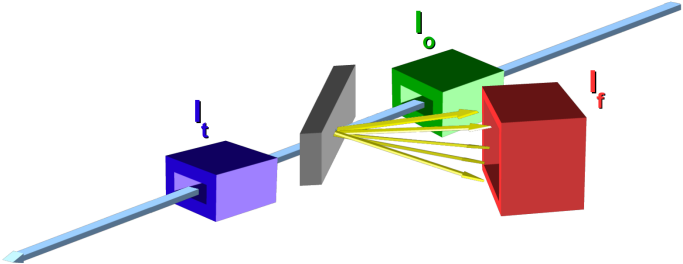

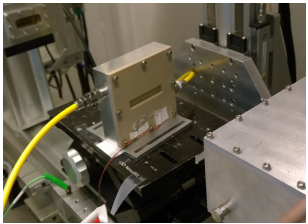

$$\mu(E) \propto \ln\left(\frac{I_o}{I_t}\right) \propto \frac{I_f}{I_o}$$

The EXAFS experiment

I_o = incident intensity
I_t = transmitted intensity
I_f = fluorescence intensity
$\mu(E)$ = absorption coefficient

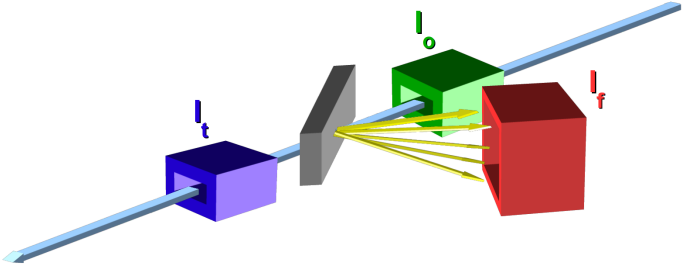

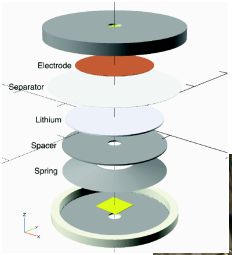

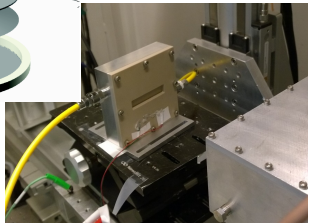

$$\mu(E) \propto \ln\left(\frac{I_o}{I_t}\right) \propto \frac{I_f}{I_o}$$

The EXAFS experiment

I_o = incident intensity
I_t = transmitted intensity
I_f = fluorescence intensity
$\mu(E)$ = absorption coefficient

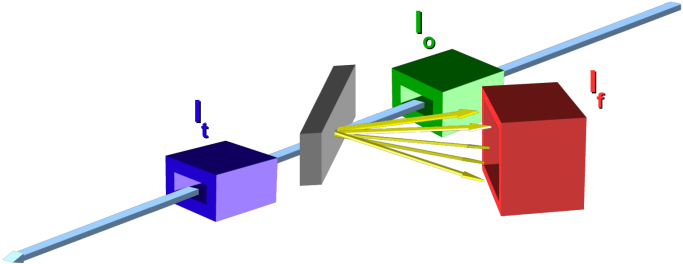

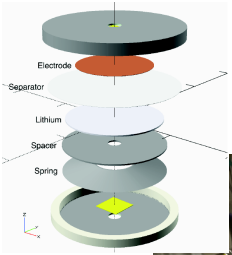

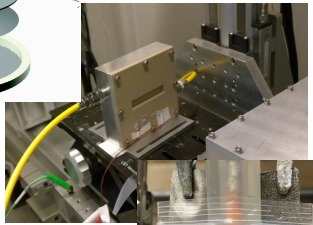

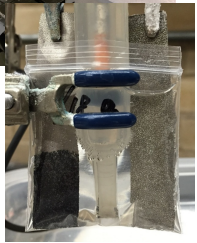

$$\mu(E) \propto \ln\left(\frac{I_o}{I_t}\right) \propto \frac{I_f}{I_o}$$

The EXAFS experiment

I_o = incident intensity
I_t = transmitted intensity
I_f = fluorescence intensity
$\mu(E)$ = absorption coefficient

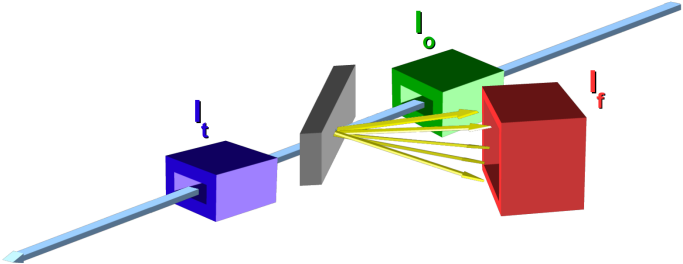

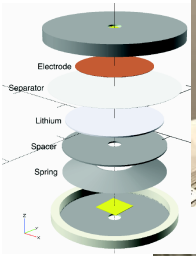

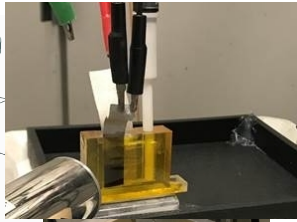

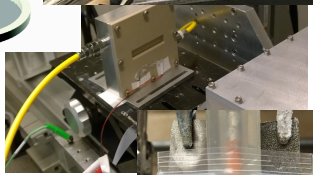

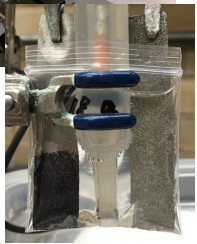

$$\mu(E) \propto \ln\left(\frac{I_o}{I_t}\right) \propto \frac{I_f}{I_o}$$

The EXAFS experiment

I_o = incident intensity
I_t = transmitted intensity
I_f = fluorescence intensity
$\mu(E)$ = absorption coefficient

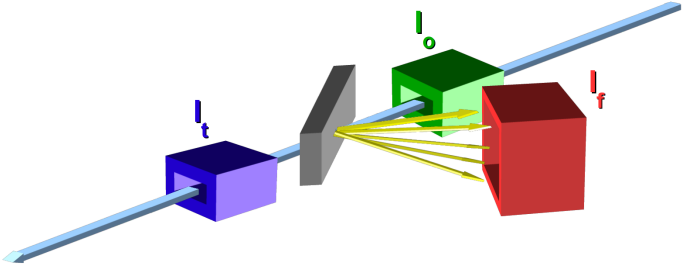

$$\mu(E) \propto \ln\left(\frac{I_o}{I_t}\right) \propto \frac{I_f}{I_o}$$

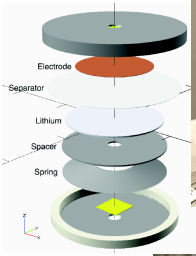

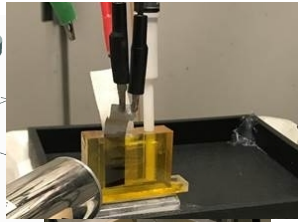

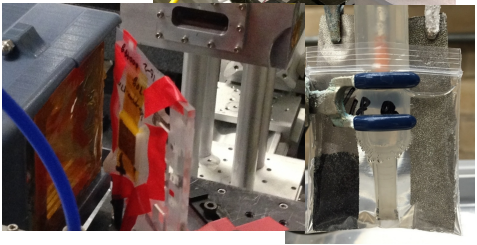

EXAFS overview

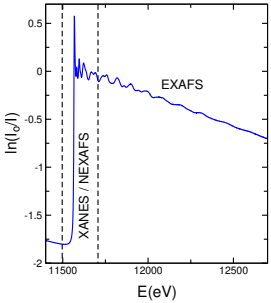

EXAFS overview

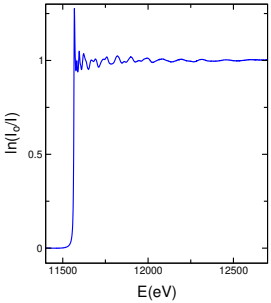

EXAFS overview

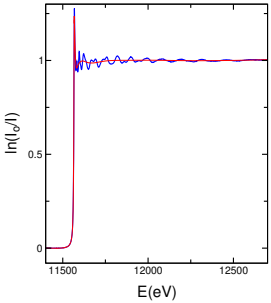

EXAFS overview

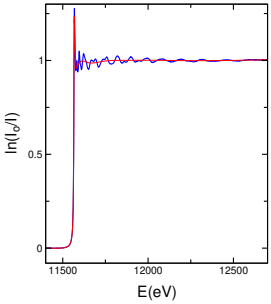

remove back-ground

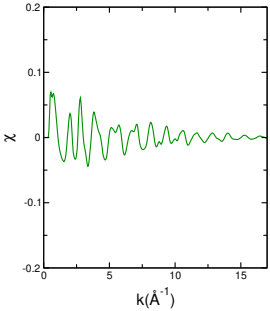

EXAFS overview

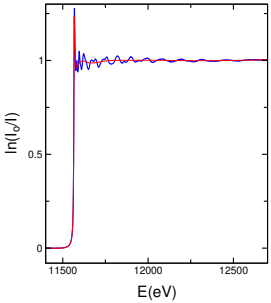

remove back-ground

apply k-weight

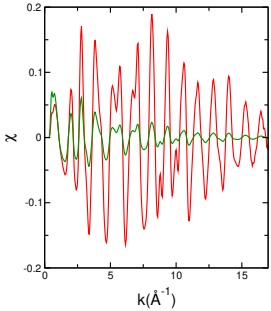

EXAFS overview

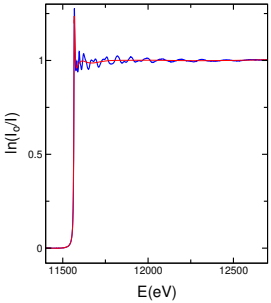

remove back-ground

apply k-weight

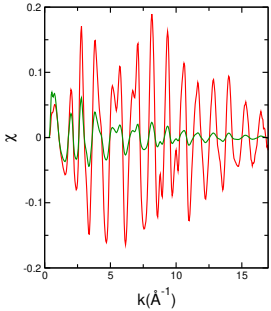

Fourier Transform

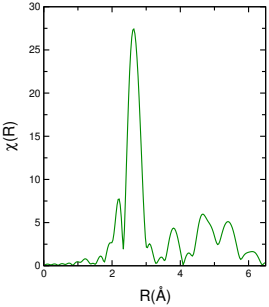

EXAFS overview

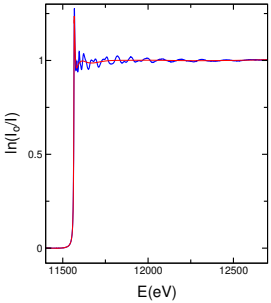

remove back-ground

apply k-weight

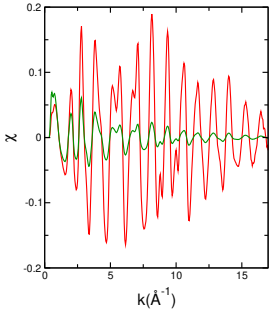

Fourier Transform

fit one

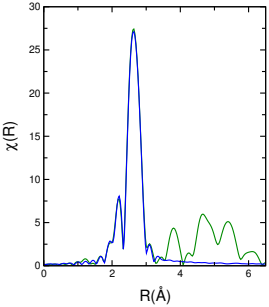

$$\chi(k) = \sum_j \frac{N_j f_j(k) e^{-2R_j/\lambda(k)} e^{-2k^2\sigma_j^2}}{k R_j^2} \sin[2kR_j + \delta_j(k)]$$

EXAFS overview

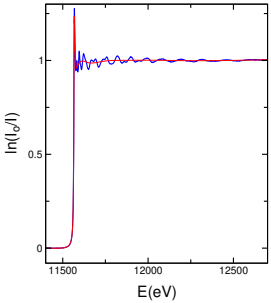

remove back-ground

apply k-weight

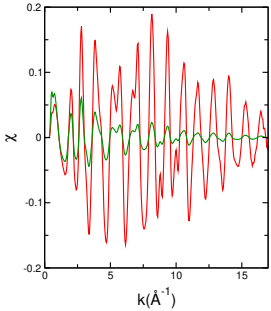

Fourier Transform

fit one or more paths

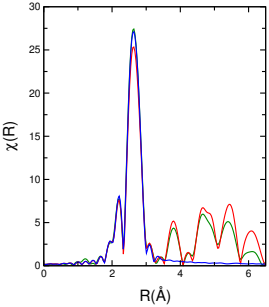

$$\chi(k) = \sum_j \frac{N_j f_j(k) e^{-2R_j/\lambda(k)} e^{-2k^2\sigma_j^2}}{k R_j^2} \sin[2kR_j + \delta_j(k)]$$

Determine Z, R, N, and σ^2 from model with computed $f(k)$, $\delta(k)$, and $\lambda(k)$

Battery chemistries accessible to XAFS

Cathode materials:

- $Ni(OH)_2@Co(OH)_2$
- MnO_2
- $LiCoO_2$
- $Li_{1.2}(NiMnCo)_{0.8}O_2$
- $Li_{1.2}(MnNiFe)_{0.8}O_2$
- $Li_3V_2(PO_4)_3$
- $LiFePO_4$

Edge	Energy
Li	0.055 keV
V	5.465 keV
Mn	6.539 keV
Fe	7.112 keV
Co	7.709 keV
Ni	8.333 keV

Li edge not directly accessible and 3d elements must be measured in fluorescence for *in situ* experiments.

Anode materials:

- Fe_2O_3
- ZnO
- MoS_2
- Sn
- SnO_2
- Sn_4P_3

Edge	Energy
P	2.145 keV
S	2.472 keV
Fe	7.112 keV
Zn	9.659 keV
Mo	20.00 keV
Sn	29.20 keV

P and S edges too low for non-vacuum experiments, Zn good in fluorescence, Mo and Sn ideal for *in situ* experiments.

$Li_{1.2}Mn_{0.5}Ni_{0.2}Fe_{0.1}O_2$ cathode

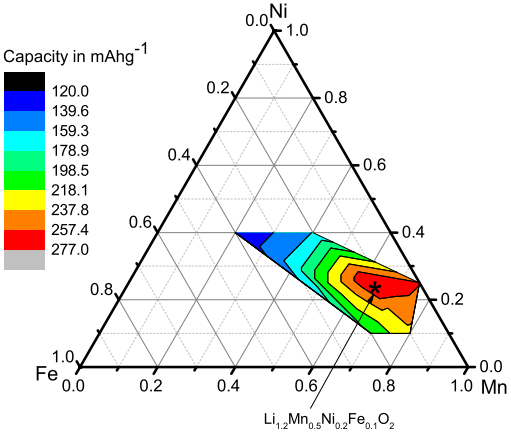

Choose composition from literature reports

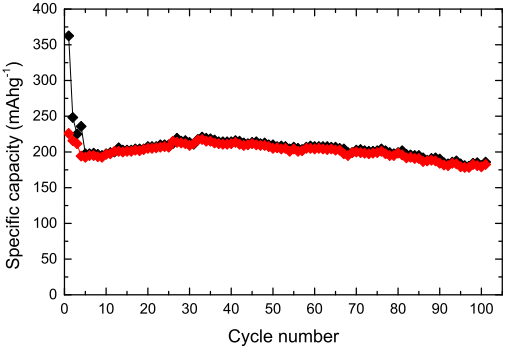

Sol-gel synthesized nanoparticles maximum capacity for 4.8 V cycling

$Li_{1.2}Mn_{0.5}Ni_{0.2}Fe_{0.1}O_2$ structure

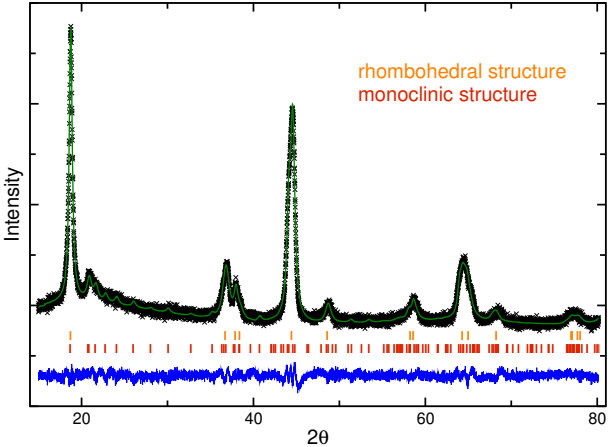

best fit requires both structures

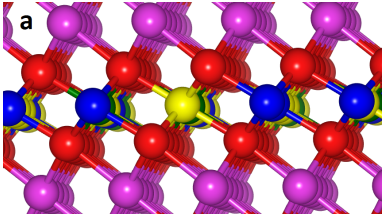

$LiCoO_2$-like rhombohedral

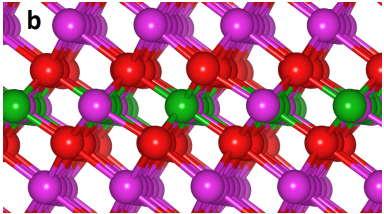

Li_2MnO_3 monoclinic

$Li_{1.2}Mn_{0.5}Ni_{0.2}Fe_{0.1}O_2$ ex situ EXAFS

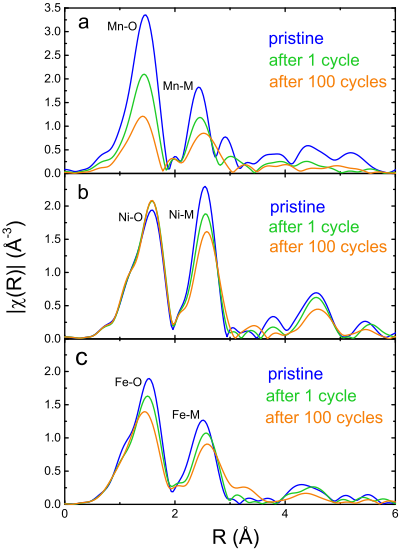

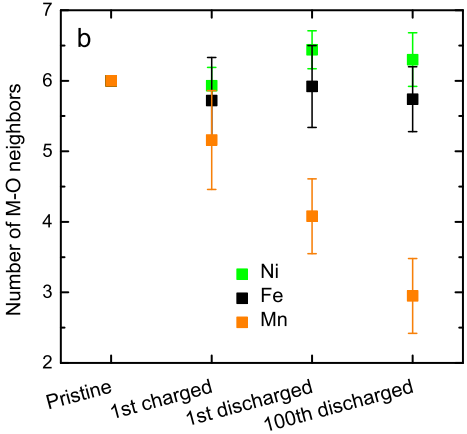

S. Aryal et al., "Structural studies of capacity activation and reduced voltage fading in Li-rich, Mn-Ni-Fe composite oxide cathode," *J. Electrochem. Soc.* **165**, A71-A78 (2018)

$Ni(OH)_2$@$Co(OH)_2$ templating

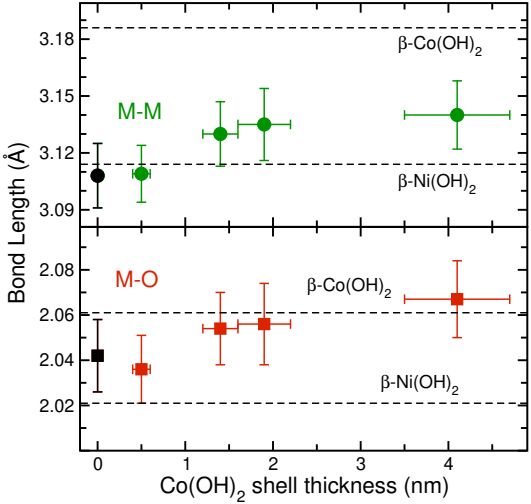

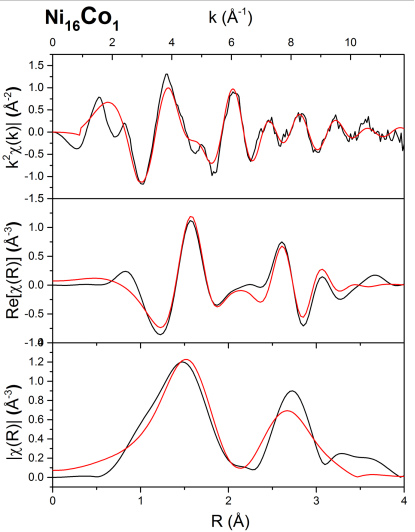

$Ni(OH)_2$@$Co(OH)_2$ templating

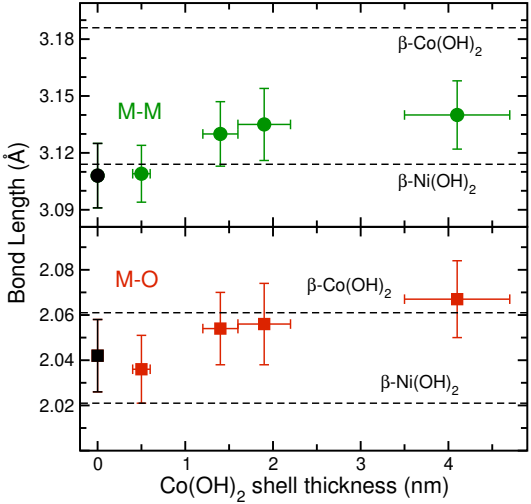

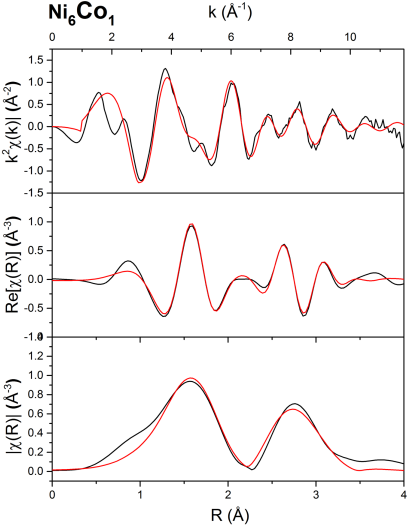

$Ni(OH)_2$@$Co(OH)_2$ templating

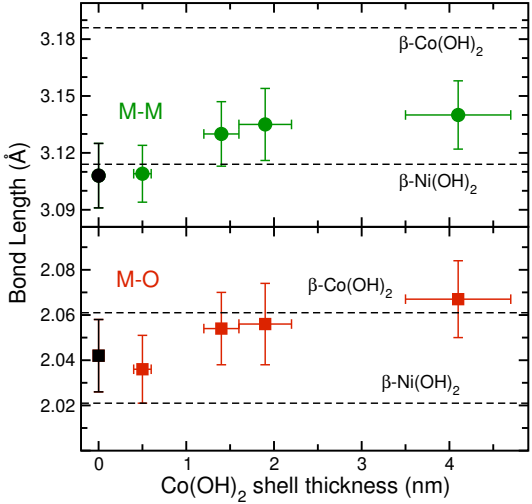

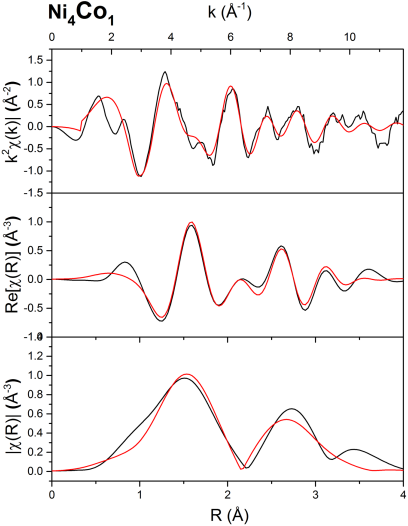

$Ni(OH)_2$@$Co(OH)_2$ templating

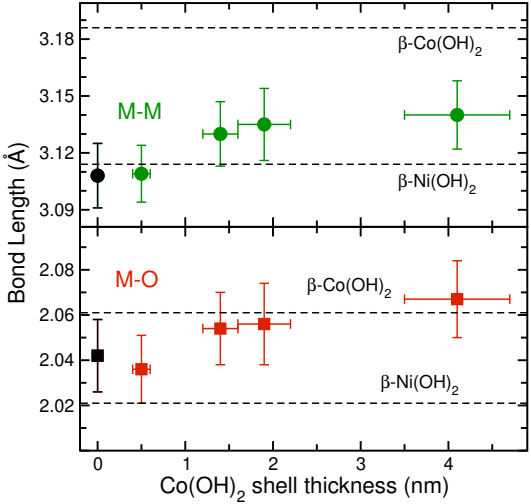

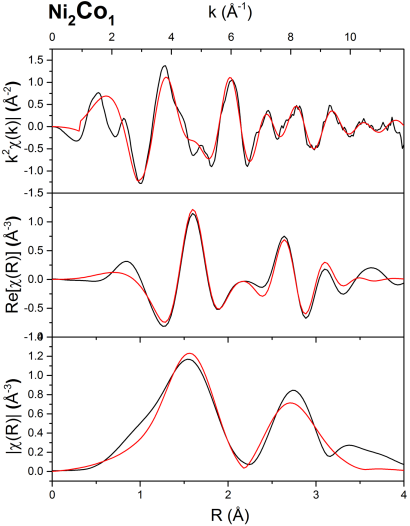

$Ni(OH)_2@Co(OH)_2$ in situ XANES

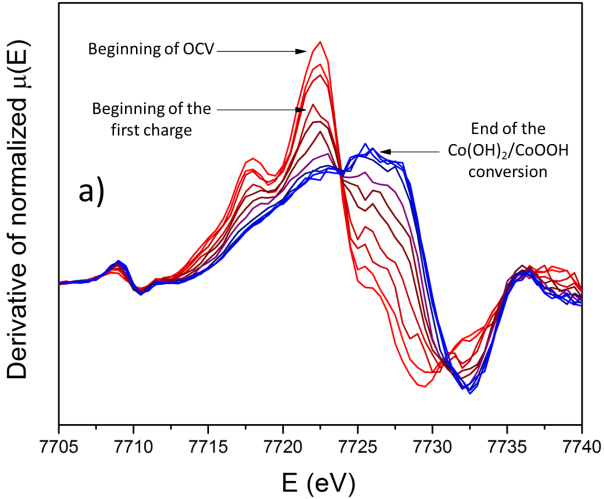

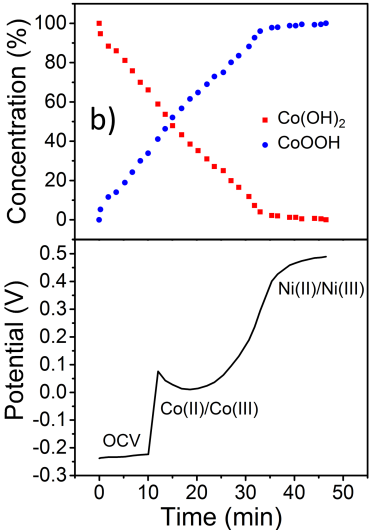

$Ni(OH)_2@Co(OH)_2$ in situ EXAFS

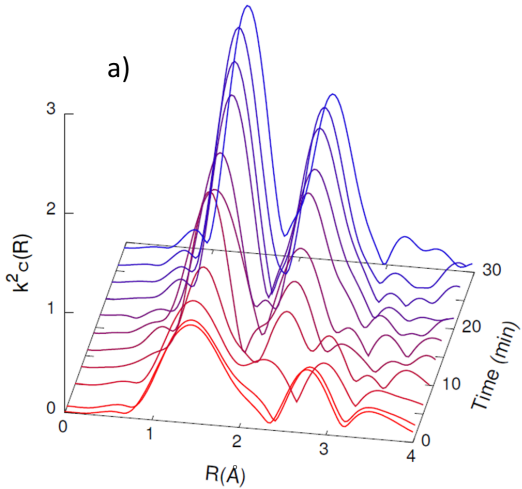

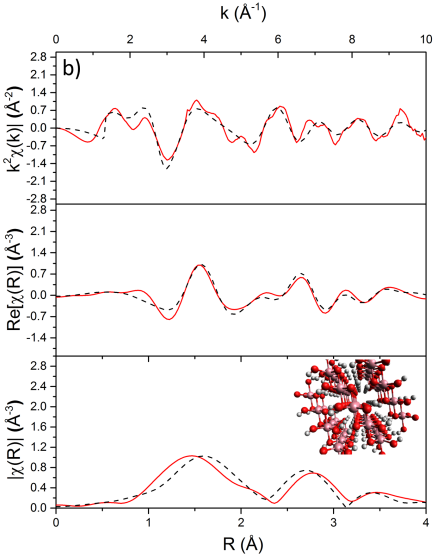

$Ni(OH)_2@Co(OH)_2$ in situ EXAFS

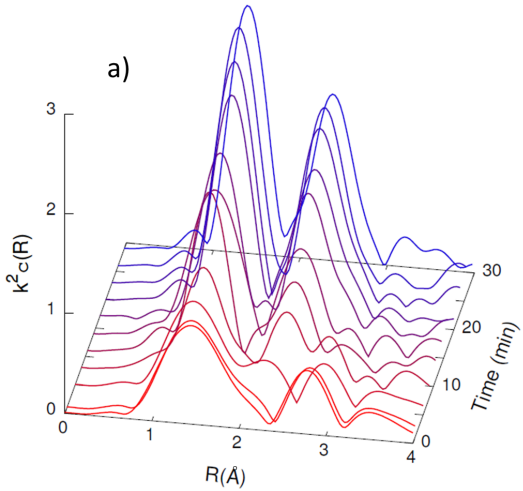

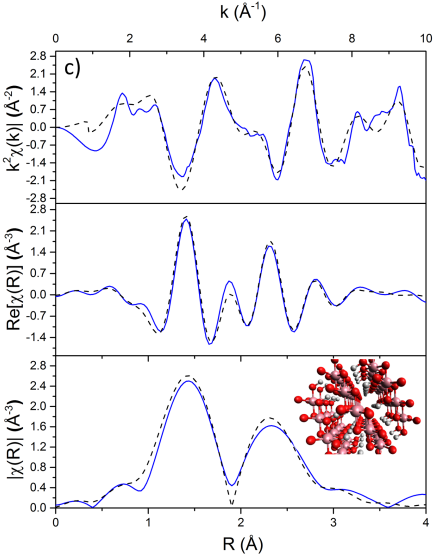

$Ni(OH)_2$@$Co(OH)_2$ galvanic couple

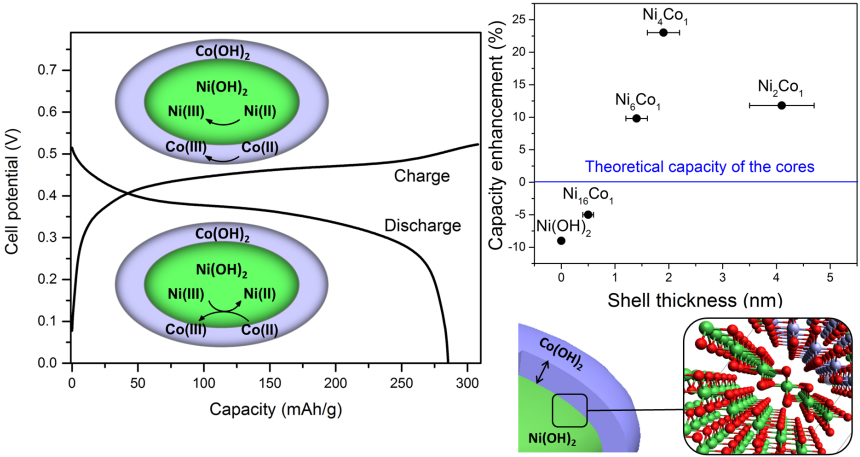

E. Moazzen et al., "Role of crystal lattice templating and galvanic coupling in enhanced reversible capacity of Ni(OH)2/Co(OH)2 core/shell battery cathode," *Electrochim. Acta* **258**, 684-693 (2017).

Sn_4P_3/graphite composite anode

Pure Sn_4P_3 synthesized by high energy ball milling, then ball milled with graphite to obtain composite

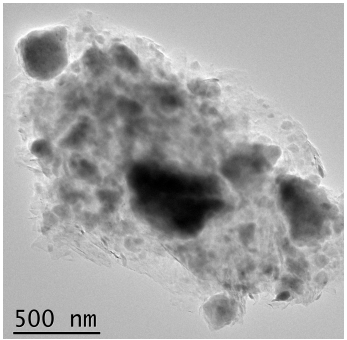

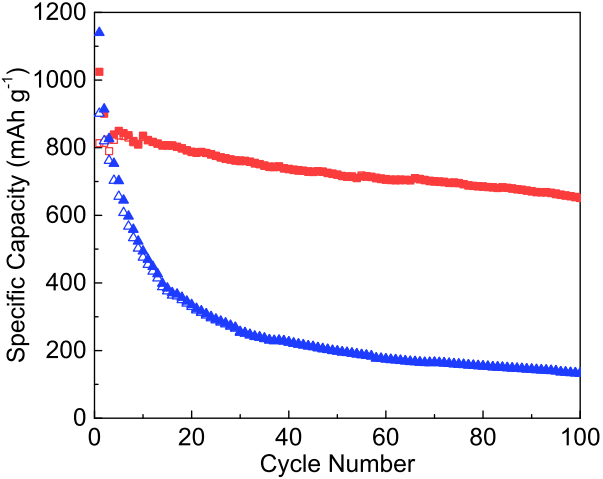

Theoretically 9+ electrons per formula unit

Third cycle comparison

Third lithiation, third delithiation, and 100th delithiation: clear difference between pure Sn_4P_3 and the Sn_4P_3/graphite composite

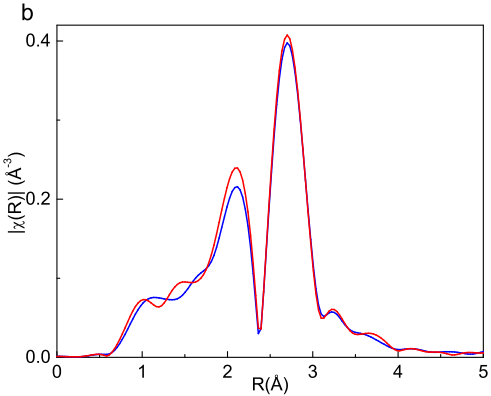

pure Sn_4P_3

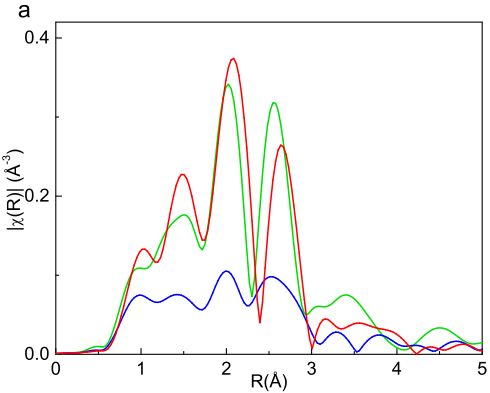

Sn_4P_3/graphite composite

Example fits

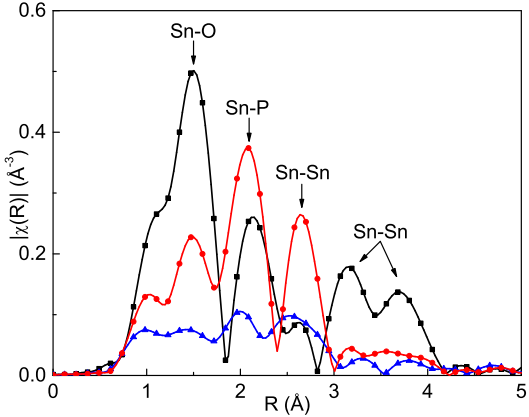

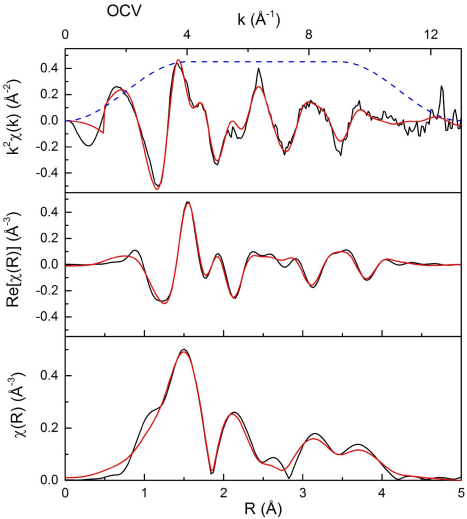

Sn_4P_3/graphite electrode at OCV, 3rd lithiation, and 3rd delithiation

Example fits

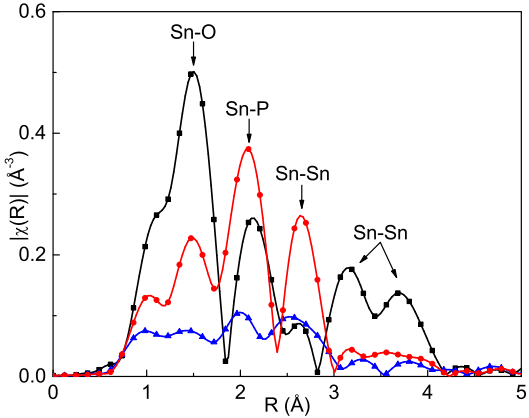

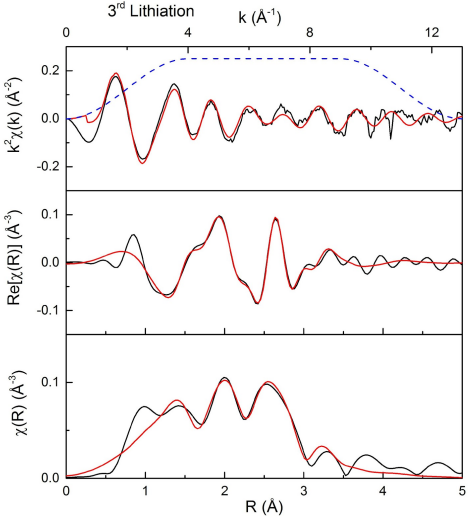

Sn_4P_3/graphite electrode at OCV, 3rd lithiation, and 3rd delithiation

Example fits

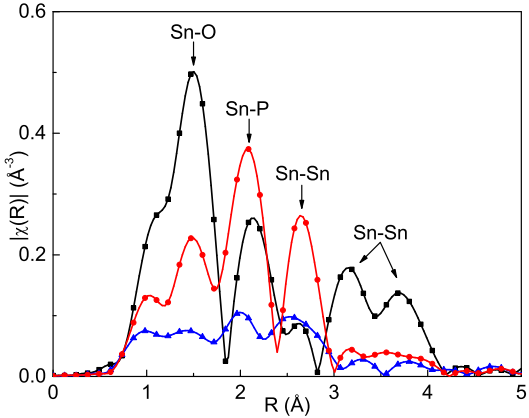

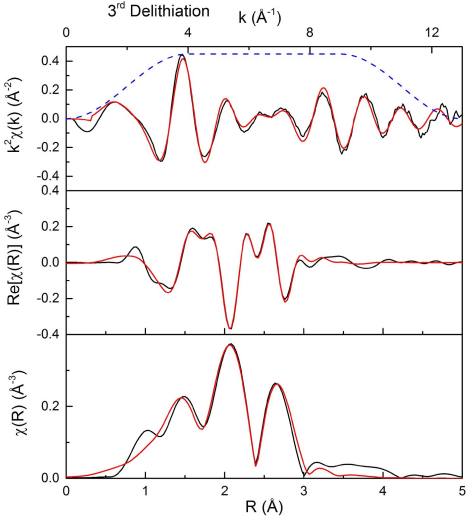

Sn_4P_3/graphite electrode at OCV, 3rd lithiation, and 3rd delithiation

Sn_4P_3/graphite fit results

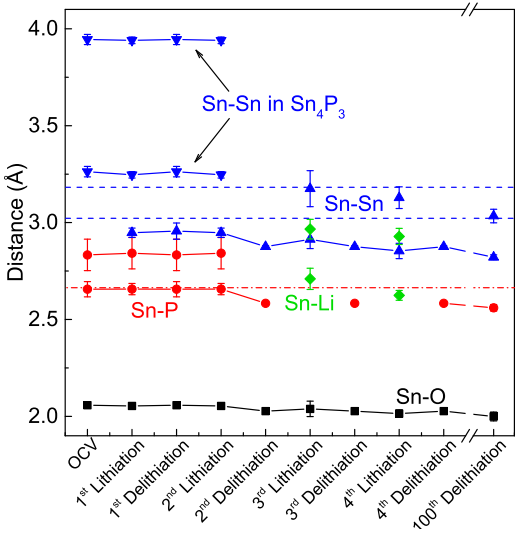

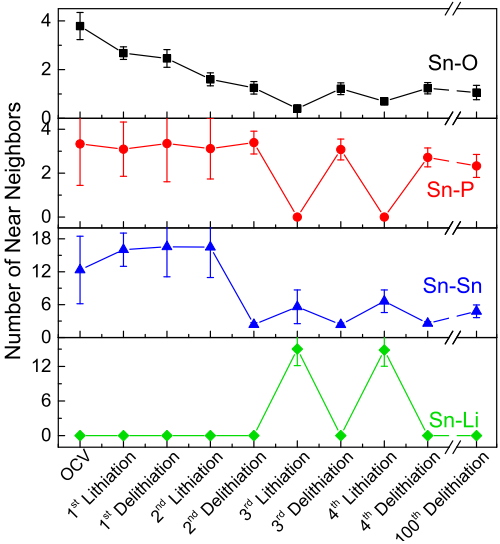

Third cycle dynamic snapshot

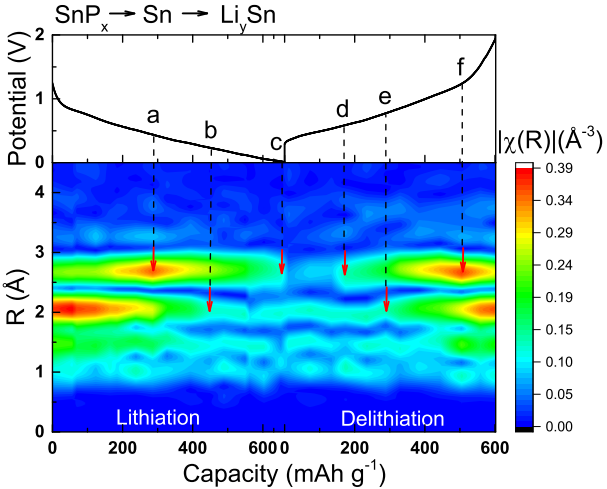

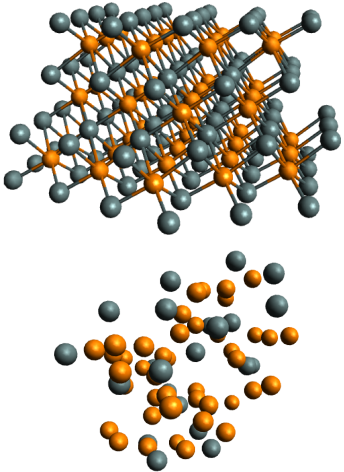

Y. Ding et al., "In situ EXAFS-derived mechanism of highly reversible tin phosphide/graphite composite anode for Li-ion batteries," *Adv. Energy Mater.* **2017**, 1702134 (2017).

Collaborators & Acknowledgements

Elena Timofeeva – Illinois Tech

Sn_4P_3/graphite composite

Yujia Ding – Illinois Tech
Zhefei Li – Ohio University

Ni@Co core-shell aqueous cathode

Elahe Moazzen – Illinois Tech

$Li_{1+x}(MnNiFe)_{1-x}O_2$ cathode materials

Shankar Aryal – Illinois Tech

Duchossois Leadership Program at Illinois Tech